

MATHEMATICAL DEVELOPMENT AND NUMERICAL ANALYSIS OF FURTHER TRANSPORT EQUATIONS FOR THE DROPLET SIZE MOMENT THEORY

Bo Yue, A. Paul Watkins

Department of Mechanical, Aerospace and Manufacturing Engineering, UMIST
Manchester, M60 1QD, United Kingdom, Tel: [44] (0) 161 200 3706
b.yue@postgrad.umist.ac.uk, paul.watkins@umist.ac.uk

ABSTRACT

This paper deals with extensions to the spray model of Beck and Watkins [1,2]. In their model, the moments of the droplet size distribution function are employed to characterize the spray. Transport equations are written for two moments that represent the liquid volume Q_3 and surface area Q_2 , along with their respective moment-averaged momentum equations. In most cases the comparisons of the results with experimental data show that this model performs well. For a number of reasons, the equations need values for the two moments Q_1 and Q_0 , representing total radius and droplet number. These are estimated in the Beck and Watkins model from an assumed size distribution function, truncated to fit the local value of Sauter mean radius, itself evaluated from Q_3 and Q_2 . This paper presents a new model in which all four moment are evaluated from transport equations, thus allowing the form of the size distribution function to be determined from the values of the moments. Different momentum equations are solved for each moment-averaged velocity component. Preliminary results indicate that the model is working as expected, but there are numerical problems to be overcome before the full model can be activated.

INTRODUCTION

The method of using moments of droplet size distributions to model sprays was first introduced by Beck and Watkins [1,2]. In this model, transport equations are written for Q_3 and Q_2 the two moments that represent the liquid volume and surface area. The velocities, U_{13} and U_{12} , employed to convect these moments, are obtained by solving separate momentum equations for each. The other two moments, Q_1 and Q_0 , representing total radius and droplet number, are approximated from a presumed drop number size distribution function, which is allowed to vary in space and time, but which requires truncation at either the small drop size or large drop size end of the distribution, in order to match the local value of the Sauter mean radius calculated from values of Q_3 and Q_2 . The transport equations for both liquid and gaseous phases are written in Eulerian form, and coupled through source terms. These equations are solved using the finite-volume approach.

The work presented here is designed to remove, as much as is possible, the need to presume a particular distribution function for drop sizes. This is done by developing transport equations for Q_1 and Q_0 , and their respective momentum equations. Thus the liquid phase is represented by four moment transport equations and four momentum equations. The development of the sub-models for the Q_3 and Q_2 equations, and their respective momentum equations, are set out in detail in [2]. The equivalent sub-models for Q_1 and Q_0 and their momentum equations, can be obtained in precisely the same way. The details of these derivations will therefore not be given here. Instead just the results of the derivation are presented in the next section.

Although the need to prescribe a size distribution is much reduced in the current model over that of its predecessor, there are still three places in the model where such a distribution is required. These are: (i) Inlet/initial conditions: the result of primary or secondary (drop) break-up needs to be prescribed; (ii) The model is not closed: due to the form of drag model used, and its dependence on drop radii, the source terms of the momentum equations involve the moments Q_{-1} and Q_{-2} . These must be modeled in terms of higher order moments. For this to be done a size distribution is required; (iii) Drop break-up involves only part of the spray distributions, i.e. the large drops. In order to calculate the effects on the moments, integration across part of the underlying distribution is needed. This can only be done if the distribution is prescribed. However, different distributions can be prescribed for these three effects.

MATHEMATICAL MODEL

The set of moment equations ($i = 0, \dots, 3$) can be compactly represented by:

$$\frac{\partial Q_i}{\partial t} + \frac{\partial}{\partial x_j} (Q_i U_{lij}) = -S_{Q_i} \quad (1)$$

The respective momentum equations can also be written compactly as:

$$\frac{\partial}{\partial t} (Q_i U_{lij}) + \frac{\partial}{\partial x_k} (Q_i U_{lij} U_{lik}) = \frac{\partial}{\partial x_k} (Q_i \sigma_v v_l \frac{\partial U_{lij}}{\partial x_k}) - S_{U_{ij}} \quad (2)$$

In these equations, the source terms S_{Q_i} represent the effects on the moments of drop break-up, drop collisions and evaporation. The source terms $S_{U_{ij}}$ describe the effects of drag on the liquid momentums. All of these effects have been incorporated into the new model, although not all have yet been satisfactorily activated. The diffusion terms are treated the same for all momentums. This treatment is described in [2].

Gamma Distributions

In the present model the three parts of the model, as discussed above, that require a given size number distribution are modeled through Gamma distributions. The general form of the Gamma number size distribution employed here is:

$$n(r) = \frac{\alpha^k}{\Gamma(k)r_{32}^k} r^{k-1} e^{-\alpha(\frac{r}{r_{32}})} \quad (3)$$

where r_{32} is the Sauter mean radius and $\Gamma(k)$ is the Gamma function defined by the integral

$$\Gamma(k) = \int_0^{\infty} e^{-x} x^{k-1} dx \quad (4)$$

and its form for positive k is shown in Fig. 1.

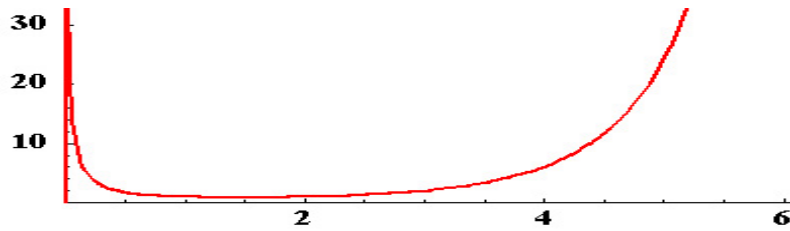


Figure 1. Gamma Function

The moments of this distribution are given by:

$$Q_i = Q_0 \int_0^{\infty} \frac{\alpha^k}{\Gamma(k)r_{32}^k} r^{k+i-1} e^{-\alpha(\frac{r}{r_{32}})} dr \quad (5)$$

By partial integration, $Q_3 = \frac{(k+2)}{\alpha} r_{32} Q_2$. By definition, $Q_3 = r_{32} Q_2$, thus $\alpha = k+2$.

$$\text{From the same analysis there also results, } Q_2 = \frac{(k+1)}{(k+2)} r_{32} Q_1, \quad Q_1 = \frac{k}{(k+2)} r_{32} Q_0 \quad (6)$$

For the calculations shown later, inlet/initial conditions are modeled by taking $k = 3.5$. This is different from the distribution as assumed throughout the Beck and Watkins model [1], which took $k = 2$. The functional forms of equ. (3) for various values of k are shown in Fig. 2.

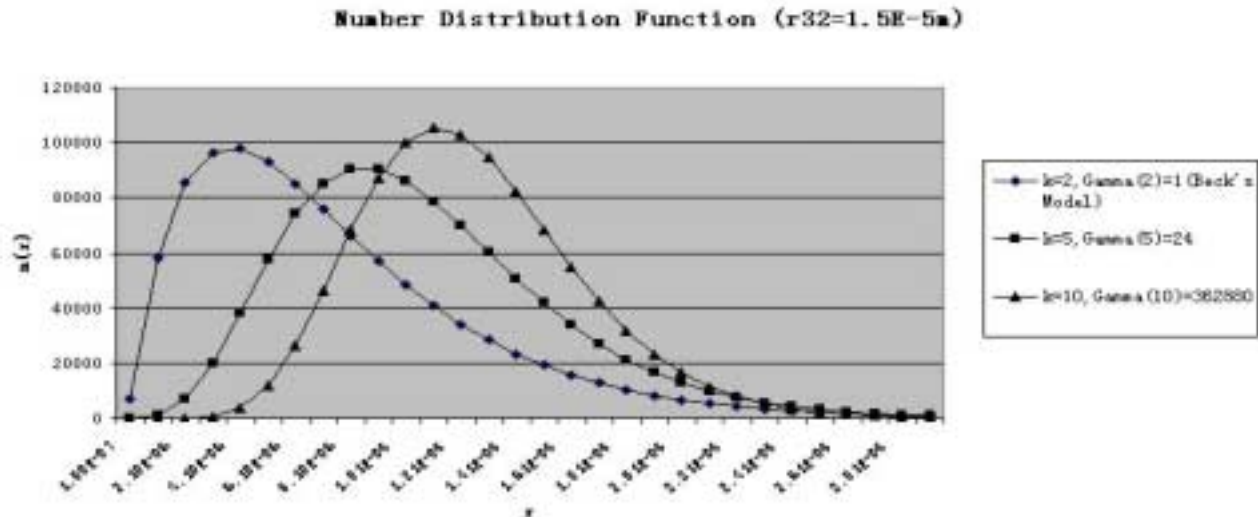


Figure 2 Gamma Distribution Function with $k = 2, 5, 10$ and $r_{32} = 15\mu\text{m}$.

For the drag model no assumption of the value of k is required. Instead equations (6) are used at each computational cell and time step to evaluate k from the calculated values of r_{32} , Q_2 , Q_1 and Q_0 . In fact, these equations over-prescribe k , as two, possibly different, values may result. Where conflict occurs, the value taken is the one nearest to the initial conditions, i.e. to 3.5 in the calculations made to date. This is to ensure numerical stability, as much as possible.

With k evaluated, integration over the size distribution yields

$$Q_{-2} = \frac{(k+2) Q_{-1}}{(k-2) r_{32}}, \quad Q_{-1} = \frac{(k+2) Q_0}{(k-1) r_{32}} \quad (7)$$

The insertion of these equations close the drag source terms in terms of known quantities. The presence of the $k-2$ term in the denominator of the Q_{-2} equation introduces numerical problems if the k value falls too close to 2. It is for this reason that the initial value of $k = 3.5$ has been chosen.

Truncated Gamma Distribution

The break-up source terms require integration across part of the size distribution for drops with radii above a critical value r_c to obtain truncated forms of Q_i ($i = -1, \dots, 2$). Thus

$$Q_{i,c} = Q_0 \int_{r_c}^{\infty} \frac{(k+2)^k}{\Gamma(k) r_{32}^k} r^{k+i-1} e^{-(k+2)\frac{r}{r_{32}}} dr = Q_0 \left(1 - \int_0^{r_c} \frac{(k+2)^k}{\Gamma(k) r_{32}^k} r^{k+i-1} e^{-(k+2)\frac{r}{r_{32}}} dr\right) \quad (8)$$

With the substitution $(k+2)\frac{r}{r_{32}} = u$, $dr = \frac{r_{32}}{k+2} du$, $u_c = (k+2)\frac{r_c}{r_{32}}$

$$Q_{0,c} = Q_0 \int_{u_c}^{\infty} \frac{(k+2)^k}{r_{32}^k \Gamma(k)} \frac{r_{32}^{k-1}}{(k+2)^{k-1}} u^{k-1} e^{-u} \frac{r_{32}}{k+2} du = Q_0 \left(1 - \int_0^{u_c} \frac{1}{\Gamma(k)} u^{k-1} e^{-u} du\right) \quad (9)$$

The final integral in equation (9) is the Cumulative Gamma distribution function.

For other values of i , analytical expression involving $Q_{0,c}$ can be obtained by partial integration, for example,

$$Q_{1,c} = Q_0 \frac{(k+2)^{k-1}}{\Gamma(k)} \frac{r_c^k}{r_{32}^{k-1}} e^{-(k+2)\frac{r_c}{r_{32}}} + \frac{k}{k+2} r_{32} Q_{0,c} \quad (10)$$

These equations close the break-up source terms.

The collision model requires evaluation of the probability that a drop has a size that is less than a number of different critical drop sizes. This again requires the Cumulative Gamma function.

Evaluation of the Cumulative Gamma Function

To evaluate the expressions in eqs. (9) and (10), values of the Cumulative Gamma function must be tabulated as a function of k and r_c . So the task is to evaluate

$$\Gamma_c(k) = \int_0^{u_c} \frac{1}{\Gamma(k)} u^{k-1} e^{-u} du \quad (11)$$

For value of u_c in the range $0 < u_c < \infty$, and for general values of $k > 1$, partial integration of equ. (11) yields

$$\Gamma_c(k) = \frac{-u_c^{k-1} e^{-u_c}}{\Gamma(k)} + \Gamma_c(k-1) \quad (12)$$

By further partial integrations a recursion relation is derived:

$$\Gamma_c(k) = -e^{-u_c} \left[\frac{u_c^{k-1}}{\Gamma(k)} + \frac{u_c^{k-2}}{\Gamma(k-1)} + \dots + \frac{u_c^{k-m}}{\Gamma(k-m+1)} \right] + \Gamma_c(k-m) \quad (13)$$

This recursion is stopped when $1 < k-m < 2$, because the functional form of Γ_c then varies over a much smaller range than for $0 < k-m < 1$, as shown in Fig. 1 for the full Gamma function.

Tabulation of $\Gamma_c(k)$ for $1 < k < 2$ is therefore required for a range of values of u_c . Examples are illustrated in Fig. 3. It is clear that the tabulation can usefully be truncated at $u_c = 10$.

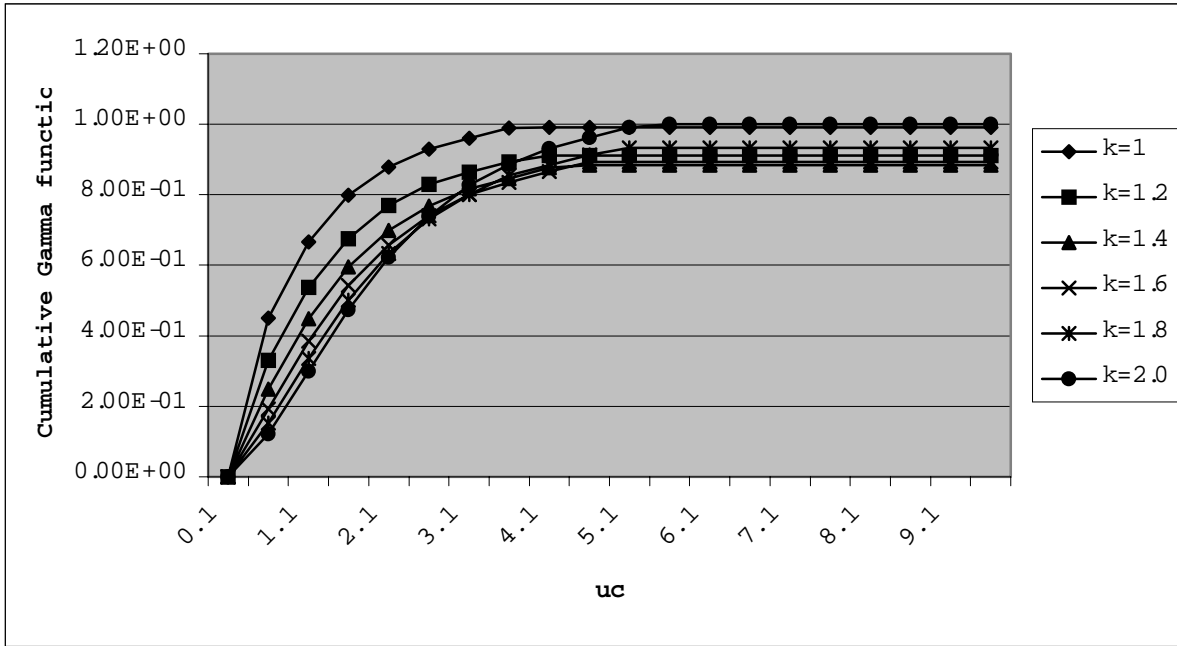
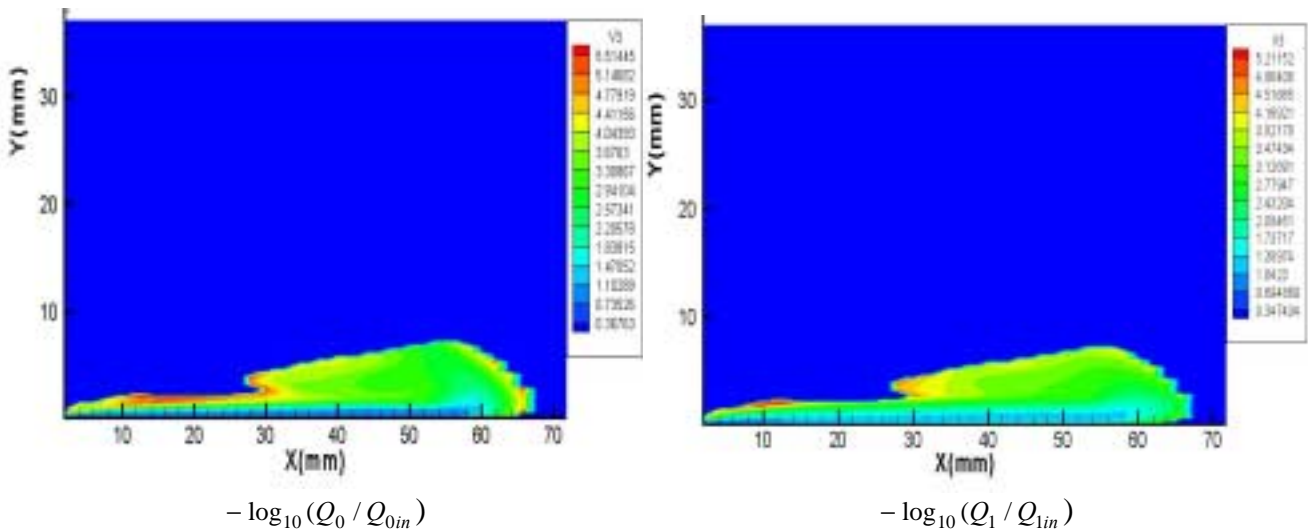


Figure 3. Cumulative Gamma Function

RESULTS

This new model was incorporated into the computer code embodying the Beck and Watkins model. This particular code is designed for a nozzle injecting a narrow axisymmetric solid-cone spray into gas. With this code, it is easy to get useful data such as penetration and width of the spray, how the drops distribute in the chamber and so on. Because of on-going numerical instabilities it is not yet possible to make a complete run of the code with the break-up sub-model activated. Thus the results illustrated here do not have drop break-up or collisions. The evaporation sub-model [3] has been extended for the new model, and incorporated into the code, but has not yet been tested.

Three cases of diesel injection into room temperature gas at elevated pressures [4] have been calculated. Figure 4 shows results for the lowest pressure case, with an injector pressure of 9.9MPa injecting into gas at 1.1MPa. The distributions of the four moments, and their corresponding velocity vectors are shown after 1000 time steps at $t=2\text{ms}$. Those for the moments are normalized by the constant inlet values, which for this case are $Q_{3in} = 0.145$, $Q_{2in} = 9.67 \times 10^3$, $Q_{1in} = 7.88 \times 10^8$ and $Q_{0in} = 8.26 \times 10^{13}$. These values are obtained in the injection cells next to the nozzle through the calculated volume fraction of liquid, giving Q_{3in} , the assumed SMR at inlet yielding Q_{2in} and the use of the prescribed Gamma distribution to give Q_{1in} and Q_{0in} .



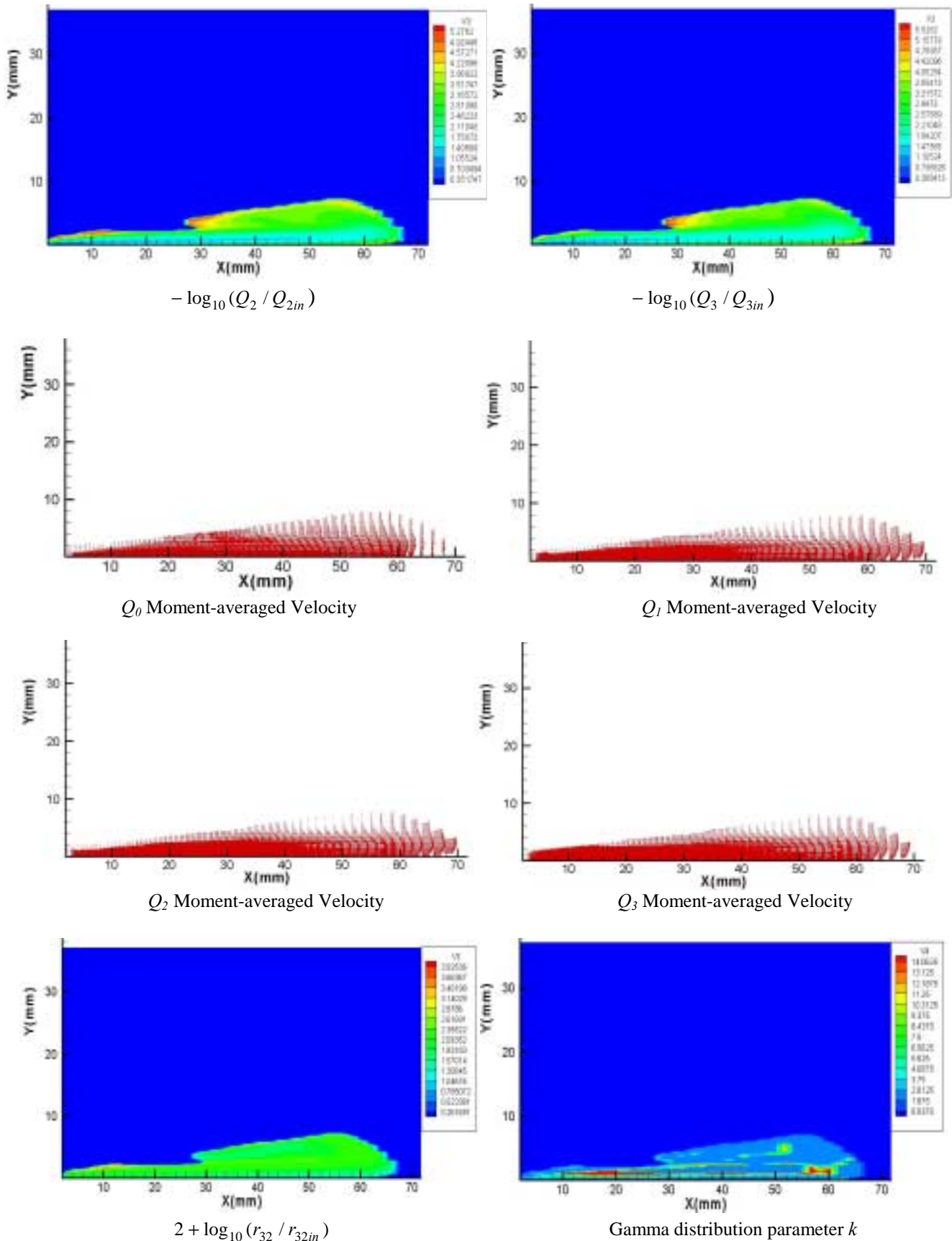


Figure 4: Field values

Note that the moment values are presented in negative log₁₀ form. This is because of the rapid dispersion of the liquid resulting in values for the moments downstream that are orders of magnitude less than at inlet. The overall structures of the distributions of the moments are relatively similar. In these calculations, none of the source terms of the moment transport

equations are active, and the same turbulent diffusion is applied to each one. Thus differences emerge only through different convection coefficients. These are different, as shown in the moment-averaged velocity fields, because the effects of drag on the moment-averaged velocities vary. For example, the volume-averaged velocity is generally larger than the surface area-averaged one reflecting the increased effect of drag on clouds of drops that are smaller in size. This phenomenon does present a numerical problem at the edges and particularly at the front of the spray. If a particular moment is convected faster than another one, there is the possibility that the former moment may appear as non-zero in a computational cell, whereas the latter remains zero. Conceptually this is not possible as the moments all relate to the same cloud of drops and therefore either all the moments are present or none are. Restrictions on the moment-averaged velocities must therefore be applied in these regions to prevent this situation occurring. However, this is not required in the body of the spray. The effects of the different moment-averaged velocities are illustrated in the final two panels in Fig. 4. The first shows the SMR. This again is presented in \log_{10} form, indicating the substantial changes occurring in the downstream spray. These changes result in both an increase in SMR in some regions, and a decrease elsewhere. The number 2 has been added to the values shown here to aid plotting by preventing negative values. Much of the spray exhibit values around 2 indicating only small changes from the inlet SMR. However, smaller values are found around the centreline illustrating the accumulation of smaller drops there as the larger drops migrate towards the edges and the front of the spray. This effect is shown by the relatively larger values found in these regions. Changes in the size distribution are also illustrated by the plot of the Gamma distribution parameter k of equ. (3). Much of the spray shows a k value that is smaller than the assumed inlet value of 3.5. This indicates that the size distribution is becoming more mono-dispersed as time progresses, due to the filtering effects of drag on the drops. The introduction of drop break-up and collision effects will undoubtedly change this picture somewhat.

Spray penetrations for the three cases examined are shown in comparison with the experimental data in Fig. 5. The comparisons are reasonable at this stage in the development of this method, although they not as good as produced by the Beck and Watkins model [1,2]. These results were produced using the same grid and time steps as results for the latter model. So either there are errors inherent in the new model, yet to be identified, or the neglect to date of drop dynamics effects are important. For example, neglect of drop break-up in the near nozzle region results in predicting too large drops on average leading to over-penetration. Conversely neglect of drop collisions downstream results in under-penetration.

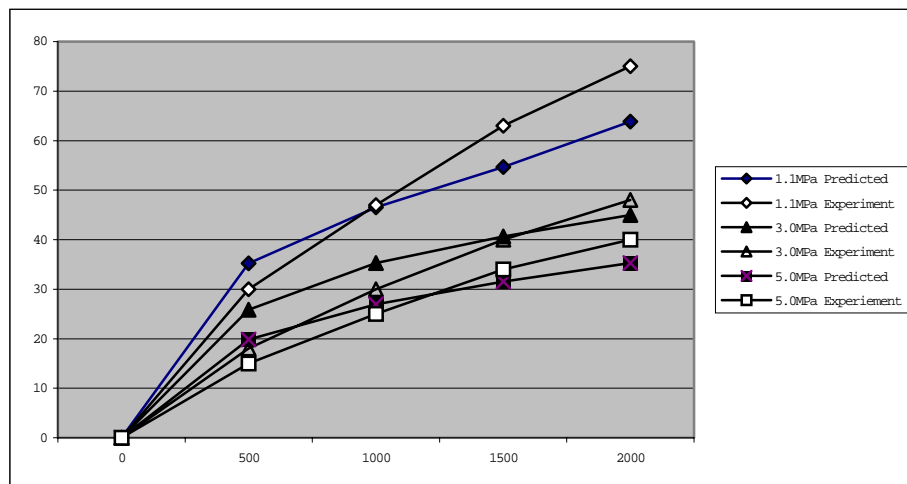


Figure 5: Spray penetration comparisons with the data of Hiroyasu and Kadota [4]

CONCLUSIONS

A new model has been developed for the simulation of poly-dispersed sprays. The model is based on using a general Gamma Distribution function for the number size distribution in order to evaluate the first four moments of the distribution and their respective moment-averaged velocities from transport equations. The model has been incorporated into a CFD code, but needs to be more rigorously tested by comparing the results with a wide range of experimental data. Although the model incorporates sub-models for heat transfer, break-up, collisions and evaporation, these aspects of the model require further research, particularly in terms of numerical stability.

REFERENCES

1. Beck, J.C., and Watkins, A.P., On the development of a spray model based on drop-size moments. *Proc. R. Soc. Lond. A*, Vol. 459, pp1365-1394, 2003
2. Beck, J.C., and Watkins, A.P., On the development of spray submodels based on droplet size moments. *J. Comput. Phys.*, 182, pp586-621, 2002
3. Beck, J.C., and Watkins, A.P., The droplet number moments approach to spray modelling: The development of heat and mass transfer sub-models. *Int. J. of Heat and Fluid Flow*, Vol. 24, No. 2, pp242-259, 2003.
4. Hiroyasu, H., and Kadota, T., Fuel droplet size distribution in diesel combustion chamber. *SAE paper 740715*, 1974.